Designer Spatial Control of Interactions in Ultracold Gases

N. Arunkumar,[1] A. Jagannathan,[1,2] and J. E. Thomas[1]
[1]Department of Physics, North Carolina State University, Raleigh, North Carolina 27695, USA
[2]Department of Physics, Duke University, Durham, North Carolina 27708, USA

(Received 2 October 2018; revised manuscript received 6 December 2018; published 1 February 2019)

Designer optical control of interactions in ultracold atomic gases has wide applications, from creating new quantum phases to modeling the physics of black holes. We demonstrate wide tunability and spatial control of interactions in a two-component cloud of ^{6}Li fermions, using electromagnetically induced transparency. With two control fields detuned $\simeq$1.5 THz from atomic resonance, megahertz changes in the frequency of one optical beam tune the measured scattering length over the full range achieved by magnetic control, with negligible (10^{-6}) effect on the net optical confining potential. A 1D "sandwich" of resonantly and weakly interacting regions is imprinted on the trapped cloud and broadly manipulated with sub-MHz frequency changes. All of the data are in excellent agreement with our continuum-dressed state theoretical model of optical control, which includes both the spatial and momentum dependence of the scattering amplitude.

DOI: 10.1103/PhysRevLett.122.040405

Tunability of interactions in ultracold atomic gases has been achieved by exploiting magnetically controlled collisional (Feshbach) resonances [1], where the total energy of two colliding atoms in an energetically open channel is tuned into resonance with a bound dimer state in a closed channel. Optical field control offers a much richer palette, by creating designer interactions with high resolution in position, energy, momentum, and time. These techniques enable new paradigms. For example, energy resolution will provide better models of neutron matter by controlling the effective range [2,3], while momentum resolution will create pairs with a nonzero center of mass momentum in two-component Fermi gases [4,5]. The increased temporal resolution enables studies of nonequilibrium thermodynamics of strongly interacting gases on timescales faster than the Fermi time [6]. Spatial manipulation of interactions can be utilized to study controllable soliton emission [7], exotic quantum phases [8], long-living Bloch oscillations of matter waves [9], the physics of Hawking radiation from black holes [10], and scale-invariant dimer pairing [11]. Optical control methods are therefore of great interest [12–19], but generally suffer from atom loss and heating due to spontaneous scattering, which severely limits their applicability.

In a major breakthrough for suppressing spontaneous scattering, Bauer *et al.* [16] used a bound-to-bound transition in the closed channel, which is far away from the atomic resonance. To further suppress atom loss, large detunings from the bound-bound transition were employed, but this limited the tunability of the scattering length a to $\Delta a \simeq 2a_{\rm bg}$, where $a_{\rm bg}$ is the background scattering length. In addition, the interaction strength was tuned by changing the intensity of the laser light, which changes the net external potential experienced by the atoms. Cetina *et al.* [17] avoided this problem by changing the spot size synchronously with the intensity to maintain a constant potential. Clark and co-workers [18] employed a "magic" wavelength approach for ^{133}Cs atoms, by tuning the control beam between the $D1$ and $D2$ lines, to suppress the atomic polarizability and hence the change in the external potential, but achieved a tunability of only $\simeq 0.2a_{\rm bg}$. This technique is applicable for well-separated optical transitions, but is not applicable to species such as ^{6}Li, where the $D1$ and $D2$ lines are closely spaced.

Recently, we demonstrated new two-field optical techniques [2,3], employing electromagnetically induced transparency (EIT) [20] in the closed channel to control magnetic Feshbach resonances [21,22]. Our technique [21] tunes the scattering length near a two-photon resonance, where the loss is at a minimum and tunability of scattering length is at a maximum, in contrast to single-field optical methods [16,18], where the maximum tunability in the scattering length is associated with maximum loss. Further, our method enables frequency tuning, where changes in one optical frequency by a few megahertz (small compared to the detuning $\approx$1.5 THz from the atomic resonance) widely tunes the scattering length, with a negligible change in the net external potential experienced by the atoms, making the method broadly applicable.

In this Letter, we report optical frequency tuning of the s-wave scattering length a near the narrow Feshbach resonance in ^{6}Li, by up to $\Delta a \simeq 12a_{\rm bg}$, where $a_{\rm bg} = 62a_0$ is the background scattering length, with a_0 the Bohr radius. We show that our optical method achieves the same tuning range as for magnetic control, which is limited only by the width of the energy distribution, due to

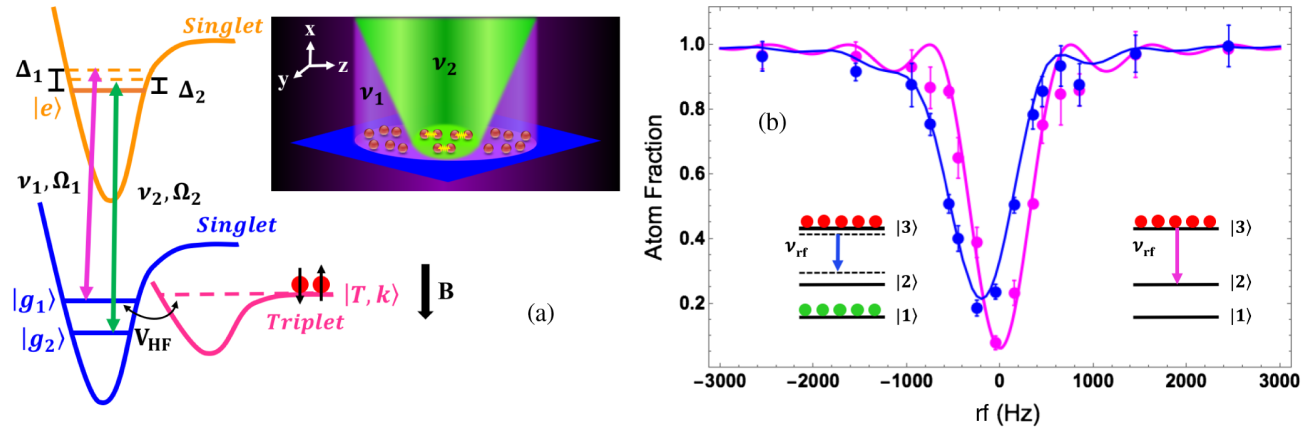

FIG. 1. Basic level scheme to control interactions using electromagnetically induced transparency (EIT). (a) Optical fields ν_1 (Rabi frequency Ω_1 and detuning Δ_1) and ν_2 (Rabi frequency Ω_2 and detuning Δ_2) couple the ground molecular states $|g_1\rangle$ and $|g_2\rangle$ to the excited molecular state $|e\rangle$ of the singlet potential, allowing precise tuning of the state $|g_1\rangle$ from below ($\delta < 0$) to above ($\delta > 0$) its unshifted position, where $\delta = \Delta_2 - \Delta_1$ is the two-photon detuning. Inset: Optical field arrangement for creating an interaction "sandwich." The central region of the atomic cloud illuminated by both ν_1 and ν_2 beams is resonantly interacting. The outer regions of the atomic cloud illuminated *only* by the ν_1 beam are weakly interacting. (b) Measuring mean-field interactions using rf spectroscopy. Fraction of atoms remaining in state $|3\rangle$ by applying a rf π pulse (1.2 ms) to transfer atoms from hyperfine state $|3\rangle$ to $|2\rangle$, obtained with (blue) and without (magenta) atoms present in state $|1\rangle$. Solid curves are predictions (see text).

the momentum dependence of the narrow Feshbach resonance [23]. Exploiting this wide tunability, we demonstrate spatial control of interactions by creating an interaction "sandwich," where the central region of the atomic cloud is resonantly interacting with $\Delta a > 10 a_{\rm bg}$ and is surrounded by two weakly interacting regions, where $\Delta a \simeq 1 a_{\rm bg}$.

Our basic method is shown in Fig. 1(a). Optical fields ν_1 (Rabi frequency Ω_1 and detuning Δ_1) and ν_2 (Rabi frequency Ω_2 and detuning Δ_2) couple the ground molecular states of the singlet potential, $|g_1\rangle$ and $|g_2\rangle$, to the excited state $|e\rangle$, tuning the energy of $|g_1\rangle$ with suppressed optical scattering [21,22]. The lowest two hyperfine states in ^{6}Li, $|1\rangle$ and $|2\rangle$, have an energy-dependent narrow Feshbach resonance (width $\Delta B = 0.1$ G) at $B_{\rm res} = 543.27$ G [23], where the atoms are predominantly in the spin triplet state $|T,k\rangle$, which tunes downward with magnetic field B as $-2\mu_B B$, where μ_B is the Bohr magneton. The triplet continuum $|T,k\rangle$ is coupled to state $|g_1\rangle$ with a second order hyperfine coupling constant $V_{\rm HF}$, which causes the narrow Feshbach resonance. For our experiments [24], $\Omega_1 = 0.5\gamma_e$ and $\Omega_2 = 2.2\gamma_e$, where $\gamma_e = 2\pi \times 11.8$ MHz is the decay rate of the excited molecular state. The detuning $\Delta_1 = +2\pi \times 19$ MHz. We define the two-photon detuning $\delta = \Delta_2 - \Delta_1$, which is varied by changing the frequency of the ν_2 laser and holding the frequency of the ν_1 laser constant. $\delta \equiv 0$ is the two-photon resonance corresponding to minimum loss. For $\delta \equiv 0$, the state $|g_1\rangle$ also returns to its original unshifted position. The state $|g_1\rangle$ is below (above) its unshifted position for $\delta < 0$ ($\delta > 0$).

We first use radio frequency spectroscopy to demonstrate optical tuning of interactions as a function of the two-photon detuning δ. To avoid three-body inelastic loss near the narrow $|1\rangle - |2\rangle$ resonance [23], we initially prepare a $|1\rangle - |3\rangle$ mixture [24], Fig. 1(b), before ramping the magnetic field to $B = B_{\rm res} + 0.010$ G. Then we apply the ν_2 beam and wait 50 ms for the atoms to reach equilibrium in the combined potential created by the ν_2 beam and the CO_2 laser trap, with a typical Fermi temperature $T_F = 1.4$ μK. The ν_1 beam is then applied concurrently with a rf π pulse (1.2 ms) that transfers atoms in state $|3\rangle$ to the initially empty state $|2\rangle$. The number of atoms remaining in state $|3\rangle$ is measured by absorption imaging as a function of the radio frequency. Figure 1(b) shows shifted (blue) and unshifted (magenta) rf spectra, obtained with and without atoms in state $|1\rangle$, respectively. The unshifted spectrum calibrates the magnetic field. The shifted spectrum is broadened due to the inhomogeneity in the atom density profile and in the intensity of the optical control beams. Figure 2(a) (red dots) shows the measured frequency shifts of the rf spectra as a function of two-photon detuning δ.

The observed frequency shifts are density dependent and arise from mean-field interactions [23,27,28] of atoms in states $|3\rangle$ and $|2\rangle$ with atoms in state $|1\rangle$, where $n_1(\mathbf{r})$ is the density. To understand the data, we calculate the local transition probability [24], which depends on the local mean-field shift $\Delta\nu_{\rm MF}$. For two-body scattering, neglecting atom-atom correlations [29,30],

$$\Delta\nu_{\rm MF}({\rm Hz}) = \frac{2\hbar}{m} n_1(\mathbf{r})[a_{13} - \langle a_{12}^{\rm opt}(\nu_2, \Omega_2(z))\rangle], \quad (1)$$

where m is the atom mass and $a_{13} \approx -267 a_0$ is the $|1\rangle - |3\rangle$ s-wave scattering length near 543 G, far from the $|1\rangle - |3\rangle$ broad Feshbach resonance (width $\Delta B \approx 122$ G) at 690 G

[23,31]. $\langle a_{12}^{\rm opt}\rangle$ is the real part of the momentum-averaged, optically controlled, two-body scattering amplitude calculated from the continuum-dressed state model [21,24] for the $|1\rangle - |2\rangle$ narrow Feshbach resonance. Note that $\langle a_{12}^{\rm opt}\rangle$ depends on the optical frequencies ν_1, ν_2, the magnetic field B, and the Rabi frequencies Ω_1, Ω_2, which are generally position dependent (along z in our experiments), enabling spatial control as demonstrated below.

We predict the spectra from the local probability for a transition from $|3\rangle$ to $|2\rangle$, integrated with the phase space distribution of atoms in the initial state $|3\rangle$ [24]. The predictions employ the measured Rabi frequencies, atom density, and rf pulse duration, with the temperature, which controls the momentum distribution, as the only adjustable parameter. For $T = 1.0\ \mu$K, the predicted frequency shifts, shown as the solid blue curve in Fig. 2(a), are in excellent agreement with the measurements. The error bars on the data points, estimated from the fluctuations in the magnetic field and optical frequencies, are negligible compared to the statistical error, which is smaller than the point size.

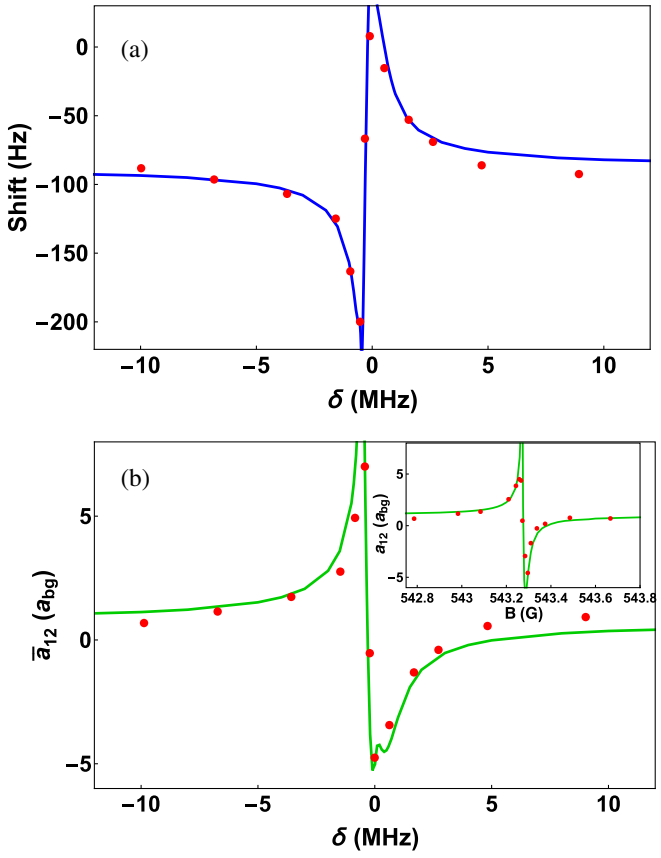

FIG. 2. Optical control of the two-body scattering length near the energy-dependent narrow Feshbach resonance of ^{6}Li at 543.27 G. (a) Measured frequency shifts in the rf spectra (red dots) and prediction (blue curve) as a function of two-photon detuning δ, by changing ν_2 and holding ν_1 constant. $\delta \equiv 0$ denotes the two-photon resonance. (b) Momentum-averaged scattering length $\bar{a}_{12}$ (red dots) determined from the measured frequency shifts versus δ and prediction (green solid curve). Inset: Magnetically tuned a_{12}. Note that optical tuning achieves the same range as magnetic tuning. $a_{bg} = 62a_0$.

The predicted two-body scattering length at $z = 0$, Fig. 2(b) green curve, is evaluated from $\langle a_{12}^{\rm opt}(\nu_2, \Omega_2(z))\rangle$ in Eq. (1), which was used to generate the predicted mean-field frequency shifts in Fig. 2(a). For comparison, we use a simple approximation to extract the scattering length $\bar{a}_{12}$ at $z = 0$, from each of the measured frequency shifts in Fig. 2(a). The $\bar{a}_{12}$, displayed as red dots in Fig. 2(b), are obtained by assuming $\Delta\nu_{\rm meas} = (2\hbar/m)\bar{n}_1(a_{13} - \bar{a}_{12})$, where $\bar{n}_1$ is a fitting parameter. We determine $\bar{n}_1$ by comparing the measured mean-field shifts with the predictions at large detunings, where the tunability of the scattering length is small. We find $\bar{n}_1 = 1.5 \times 10^{11}$ cm^{-3} [24]. As expected, $\bar{n}_1$ is smaller than the typical mean density in the experiments, $\bar{n} = 2.0 \times 10^{11}$ cm^{-3}, since the predicted scattering length is largest at $z = 0$.

Figure 2(b) shows that changing the frequency δ by just a few megahertz tunes the two-body scattering length between $+7a_{\rm bg}$ (below resonance) and $-5a_{\rm bg}$ (above resonance), the same range as obtained by magnetic tuning without optical fields, Fig. 2(b) (inset). As noted previously [23], for a narrow resonance, the effective range is large; i.e., the maximum scattering length is limited by small width $\simeq$0.1 G and the energy spread, i.e., $|a_{\rm max}/a_{\rm bg}| \simeq 2\mu_B \Delta B/\Delta E \simeq 10$, for the conditions of our experiment.

We demonstrate spatial control of two-body interactions by using the scheme of Fig. 1 (inset), where the spot sizes of the control fields are made large enough [24] to enable *in situ* images of the spatially controlled interaction profiles, as shown in Fig. 3. The two-photon detuning δ is employed as a control parameter to change the interaction spatial profiles. After illuminating the atoms with the ν_1 and ν_2 beams, we apply a rf π pulse (1.2 ms) that transfers atoms from the initial state $|3\rangle$ to state $|2\rangle$, in the presence of atoms in state $|1\rangle$. The frequency of the rf pulse is chosen to be resonant for $\delta = \pm 10$ MHz, where the entire cloud is weakly interacting.

Measured 2D absorption images of the atoms that arrive in state $|2\rangle$ are shown in Fig. 3(a) as a function of δ, where ν_2 is varied and ν_1 is held constant. The corresponding 1D axial profiles are shown in Fig. 3(c) (blue). The transferred fraction of atoms in state $|2\rangle$ depends on the spatially varying, optically controlled $|1\rangle - |2\rangle$ scattering amplitude. Figure 3(d) shows the two-body scattering length $a_{12}^{\rm opt}(z)$ used to generate the predicted 1D spatial profiles [red curves in Fig. 3(c)] and the predicted 2D absorption images in Fig. 3(b) [24].

Excellent quantitative agreement is obtained between the measured (blue) and the calculated (red) 1D axial profiles, Fig. 3(c). For the predictions, we again use the measured density and optical field parameters, and adjust the temperature, which determines the momentum distribution to be $T = 1.0\ \mu$K, the same as for Fig. 2. The asymmetry in the

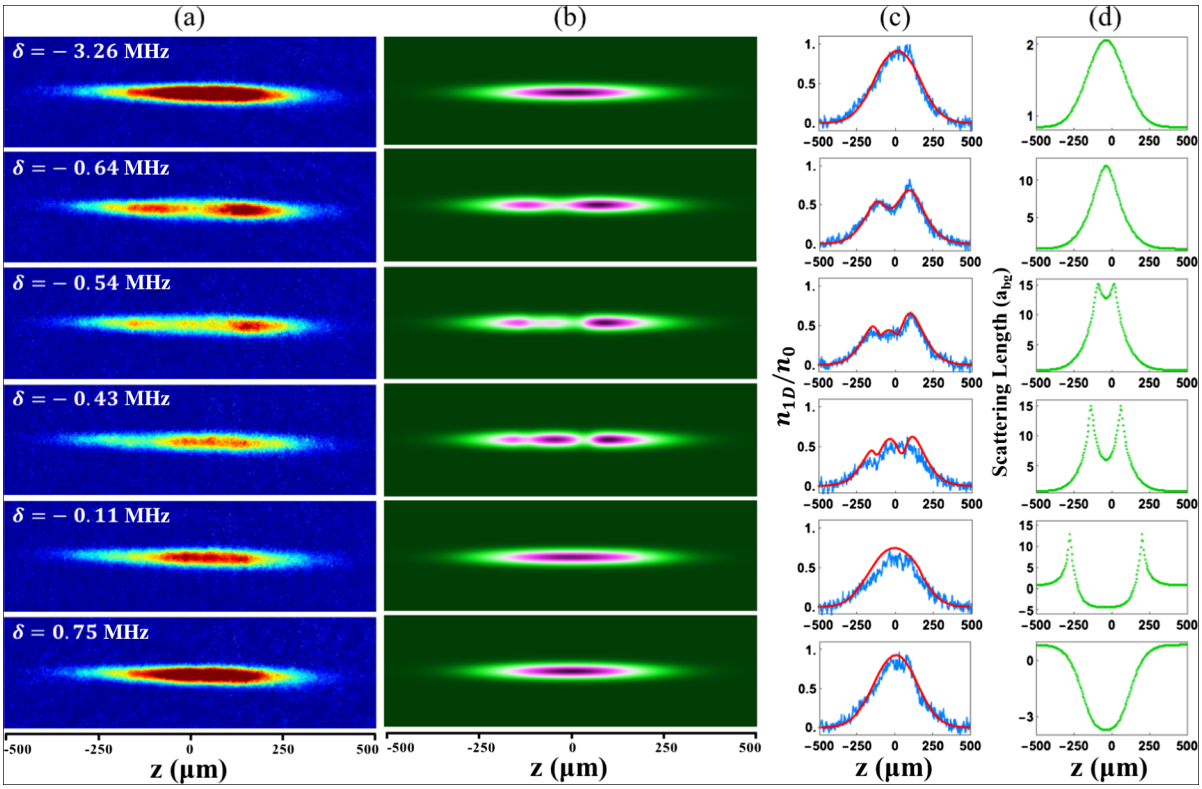

FIG. 3. Designer interaction patterns in an ultracold gas of ^{6}Li atoms versus two-photon detuning δ, with $\delta \equiv 0$ at the two-photon resonance. (a) Measured false-color 2D absorption images of atoms arriving into $|2\rangle$ after transfer from state $|3\rangle$ by a 1.2 ms rf π pulse, in the presence of atoms in state $|1\rangle$. (b) Predicted 2D images using measured parameters [24]. (c) Normalized 1D axial profiles n_{1D}/n_0, where n_0 is the peak density with no atoms in state $|1\rangle$. Measured (blue) and calculated (red). (d) Momentum-averaged two-body scattering length $a_{12}^{\rm opt}$ used to generate the predicted 2D and 1D spatial profiles.

1D profiles for $\delta = -0.64$ MHz and $\delta = -0.54$ MHz is due to the off-center position of the ν_2 beam, which is taken into account in generating the calculated 1D profiles.

At $\delta = -0.64$ MHz, we create an interaction "sandwich," where the central region of the atomic cloud is resonantly interacting with $a_{12} \approx 12 a_{\rm bg}$ and is enclosed by two weakly interacting regions with $a_{12} \approx 1 a_{\rm bg}$ [Fig. 3(d)]. This is evident from the measured 2D profile in Fig. 3(a), where the fraction of atoms transferred to state $|2\rangle$ in the central region of the cloud is heavily suppressed, due to the large frequency shift arising from resonant interactions. The measured suppression is not due to atom loss, as we observe that atoms remain in the initial state $|3\rangle$, when they are not transferred to state $|2\rangle$.

We see that a small frequency change from $\delta = -0.64$ MHz to $\delta = -0.43$ MHz inverts the interaction sandwich by making the central region more weakly interacting than the wings of the atomic cloud, resulting in increased transfer near the center, Fig. 3(a). Although the sign of the interaction is not directly evident in the 2D profiles, the predicted scattering amplitude, Fig. 3(d), shows that we can invert the sign of the 1-2 scattering length between the central and the outer regions of the cloud. For $\delta = -0.11$ MHz, the interactions in the central region become attractive with $a_{12} \approx -5 a_{\rm bg}$ and the interactions in the wings become repulsive with $a_{12} \approx 10 a_{\rm bg}$. As δ is tuned from below the two-photon resonance, $\delta = -3.26$ MHz, to above the two-photon resonance, $\delta = +0.75$ MHz, the interactions in the central region of the cloud change sign from repulsive to attractive [24]. We see that a δ tuning range of just 4 MHz imprints widely different interaction "designs" on the atomic cloud.

Previous experiments demonstrating spatial control of interactions suffered from either extremely short (10 μs) lifetimes [15] or limited optical tunability, $0.15 a_{\rm bg}$ [18]. Further, all-optical manipulation of spatial interaction profiles has not been previously demonstrated. The two-field EIT method demonstrated here provides a robust, frequency tunable method for spatiotemporal control of interactions with negligible change in the net confining potential. For the timescale (1.2 ms) and densities used in our optical control experiments, the atom loss due to spontaneous scattering is negligible [24], making this method ideal for studies of local nonequilibrium dynamics on timescales fast compared to the Fermi time [6,17], $\tau_F \simeq \hbar/E_F \simeq 10$ μs for $E_F = 5$ μK and for studies of resonantly interacting Bose gases, which exhibit hydrodynamic flow and achieve local equilibrium on millisecond timescales [32].

Our method has broad applications, creating new fields of study in ultracold gases. For example, one can imprint an interaction superlattice, where interactions between atoms at different lattice sites are independently controlled and manipulated with minimum scattering loss, permitting studies of "collisionally inhomogeneous" systems [33]. Further, a momentum selective extension of our method has been suggested as a means for realizing synthetic Fulde-Ferrell superfluids, where resonant interactions and atom pairing occur at finite momentum, with suppressed optical loss [4,5].

This research is supported by the Physics Divisions of the Air Force Office of Scientific Research (Grant No. FA9550-16-1-037) and the National Science Foundation (Grant No. PHY-1705364). Additional support is provided by the Army Research Office (Grant No. W911NF-14-1-0628) and the Division of Materials Science and Engineering, the Office of Basic Energy Sciences, Office of Science, U.S. Department of Energy (Grant No. DE-SC0008646).

[1] C. Chin, R. Grimm, P. Julienne, and E. Tiesinga, Feshbach resonances in ultracold gases, Rev. Mod. Phys. **82**, 1225 (2010).
[2] H. Wu and J. E. Thomas, Optical Control of Feshbach Resonances in Fermi Gases Using Molecular Dark States, Phys. Rev. Lett. **108**, 010401 (2012).
[3] H. Wu and J. E. Thomas, Optical control of the scattering length and effective range for magnetically tunable Feshbach resonances in ultracold gases, Phys. Rev. A **86**, 063625 (2012).
[4] J. Jie and P. Zhang, Center-of-mass-momentum-dependent interaction between ultracold atoms, Phys. Rev. A **95**, 060701 (2017).
[5] L. He, H. Hu, and X.-J. Liu, Realizing Fulde-Ferrell Superfluids via a Dark-State Control of Feshbach Resonances, Phys. Rev. Lett. **120**, 045302 (2018).
[6] A. Bulgac and S. Yoon, Large Amplitude Dynamics of the Pairing Correlations in a Unitary Fermi Gas, Phys. Rev. Lett. **102**, 085302 (2009).
[7] M. I. Rodas-Verde, H. Michinel, and V. M. Pérez-García, Controllable Soliton Emission from a Bose-Einstein Condensate, Phys. Rev. Lett. **95**, 153903 (2005).
[8] X.-L. Deng, D. Porras, and J. I. Cirac, Quantum phases of interacting phonons in ion traps, Phys. Rev. A **77**, 033403 (2008).
[9] M. Salerno, V. V. Konotop, and Yu. V. Bludov, Long-living Bloch Oscillations of Matter Waves in Periodic Potentials, Phys. Rev. Lett. **101**, 030405 (2008).
[10] R. Balbinot, A. Fabbri, S. Fagnocchi, A. Recati, and I. Carusotto, Nonlocal density correlations as a signature of Hawking radiation from acoustic black holes, Phys. Rev. A **78**, 021603 (2008).
[11] Y. Nishida and D. Lee, Weakly bound molecules trapped with discrete scaling symmetries, Phys. Rev. A **86**, 032706 (2012).
[12] F. K. Fatemi, K. M. Jones, and P. D. Lett, Observation of Optically Induced Feshbach Resonances in Collisions of Cold Atoms, Phys. Rev. Lett. **85**, 4462 (2000).
[13] K. Enomoto, K. Kasa, M. Kitagawa, and Y. Takahashi, Optical Feshbach Resonance Using the Intercombination Transition, Phys. Rev. Lett. **101**, 203201 (2008).
[14] M. Theis, G. Thalhammer, K. Winkler, M. Hellwig, G. Ruff, R. Grimm, and J. H. Denschlag, Tuning the Scattering Length with an Optically Induced Feshbach Resonance, Phys. Rev. Lett. **93**, 123001 (2004).
[15] R. Yamazaki, S. Taie, S. Sugawa, and Y. Takahashi, Submicron Spatial Modulation of an Interatomic Interaction in a Bose-Einstein Condensate, Phys. Rev. Lett. **105**, 050405 (2010).
[16] D. M. Bauer, M. Lettner, C. Vo, G. Rempe, and S. Dürr, Control of a magnetic Feshbach resonance with laser light, Nat. Phys. **5**, 339 (2009).
[17] M. Cetina, M. Jag, R. S. Lous, J. T. M. Walraven, R. Grimm, R. S. Christensen, and G. M. Bruun, Decoherence of Impurities in a Fermi sea of Ultracold Atoms, Phys. Rev. Lett. **115**, 135302 (2015).
[18] L. W. Clark, L.-C. Ha, C.-Y. Xu, and C. Chin, Quantum Dynamics with Spatiotemporal Control of Interactions in a Stable Bose-Einstein Condensate, Phys. Rev. Lett. **115**, 155301 (2015).
[19] O. Thomas, C. Lippe, T. Eichert, and H. Ott, Experimental realization of a Rydberg optical Feshbach resonance in a quantum many-body system, Nat. Commun. **9**, 2238 (2018).
[20] S. E. Harris, Electromagnetically induced transparency, Phys. Today **50**, No 7, 36 (1997).
[21] A. Jagannathan, N. Arunkumar, J. A. Joseph, and J. E. Thomas, Optical Control of Magnetic Feshbach Resonances by Closed-Channel Electromagnetically Induced Transparency, Phys. Rev. Lett. **116**, 075301 (2016).
[22] A. Jagannathan, Optical control of magnetic Feshbach resonances by closed-channel electromagnetically induced transparency, Ph.D. thesis, Duke University, 2016.
[23] E. L. Hazlett, Y. Zhang, R. W. Stites, and K. M. O'Hara, Realization of a Resonant Fermi Gas with a Large Effective Range, Phys. Rev. Lett. **108**, 045304 (2012).
[24] See Supplemental Material at http://link.aps.org/supplemental/10.1103/PhysRevLett.122.040405 for a description of the theoretical model of the frequency shifts and spatial profiles and of the experimental methods, which includes Refs. [25,26].
[25] R. Côté, Ultra-cold collisions of identical atoms, Ph.D. thesis, Massachusetts Institute of Technology, 1995.
[26] R. Côté and A. Dalgarno, Mechanism for the production of $^6Li_2$ and $^7Li_2$ ultracold molecules, J. Mol. Spectrosc. **195**, 236 (1999).
[27] S. Gupta, Z. Hadzibabic, M. W. Zwierlein, C. A. Stan, K. Dieckmann, C. H. Schunck, E. G. M. van Kempen, B. J. Verhaar, and W. Ketterle, Radio-frequency spectroscopy of ultracold fermions, Science **300**, 1723 (2003).
[28] C. A. Regal and D. S. Jin, Measurement of Positive and Negative Scattering Lengths in a Fermi Gas of Atoms, Phys. Rev. Lett. **90**, 230404 (2003).
[29] G. Baym, C. J. Pethick, Z. Yu, and M. W. Zwierlein, Coherence and Clock Shifts in Ultracold Fermi Gases

with Resonant Interactions, Phys. Rev. Lett. **99**, 190407 (2007).

[30] M. Punk and W. Zwerger, Theory of rf-Spectroscopy of Strongly Interacting Fermions, Phys. Rev. Lett. **99**, 170404 (2007).

[31] M. Bartenstein, A. Altmeyer, S. Riedl, R. Geursen, S. Jochim, C. Chin, J. H. Denschlag, R. Grimm, A. Simoni, E. Tiesinga, C. J. Williams, and P. S. Julienne, Precise Determination of ^{6}Li Cold Collision Parameters by Radio-Frequency Spectroscopy on Weakly Bound Molecules, Phys. Rev. Lett. **94**, 103201 (2005).

[32] R. J. Fletcher, J. Man, R. Lopes, P. Christodoulou, J. Schmitt, M. Sohmen, N. Navon, R. P. Smith, and Z. Hadzibabic, Elliptic flow in a strongly interacting normal Bose gas, Phys. Rev. A **98**, 011601 (2018).

[33] G. Theocharis, P. Schmelcher, P. G. Kevrekidis, and D. J. Frantzeskakis, Matter-wave solitons of collisionally inhomogeneous condensates, Phys. Rev. A **72**, 033614 (2005).